The International Journal of Advanced Manufacturing Technology (2018) 95:3045–3055
https://doi.org/10.1007/s00170-017-1393-8

ORIGINAL ARTICLE

Repair of defective 3D blade model based on deformation of adjacent non-defective cross-sectional curve

Hongying Yu[1] · Xuegeng Lyu[1]

Received: 17 July 2017 / Accepted: 13 November 2017 / Published online: 5 December 2017

Abstract
Currently, most blade repairing methods are primarily oriented for a straight or slightly curved blade; moreover, they are based on non-contact measured point-cloud, resulting in low accuracy and significant uncertainty-related issues on the defective region during repair. Therefore, this study investigates a contact measured point method with a high accuracy to analyze the repairing of a defective twisted blade; in addition, the paper proposes a new repairing method of deforming the reference cross-sectional curves adjacent to defective cross-sectional curves recursively. In order to accomplish the aforementioned, first, an interpolation algorithm of the cross-sectional curves using B-spline is set; thereafter, a criterion of the measured point density based on the size relationship between the defective region and the blade as a whole is determined. Subsequently, the registration algorithm of the reference curve and measured points of the defective cross-sectional curve to facilitate the deforming operation is provided. An iteratively moving distribution algorithm of all control points belonging to the reference curve is proposed by this paper in order to realize curve deformation. The paper presents twisted blade repairing examples and also compares the repairing surface and the designed surface to verify the validity of the proposed method. The blade repairing method proposed in this paper is aimed to guarantee a surface smooth restoration with higher accuracy and offers good conditions for several designing and repairing cases.

Keywords Defective blade repairing · 3D model · Adjacent cross-sectional curve · Curve deformation

1 Introduction

The continuous development of the machining and CAD/CAM technologies has influenced the manufacture, processing, and repairing of aero-engine blades to be developed by an automated process with high accuracy. High repairing accuracy and data sharing during repairing processes are the main problems in the current repairing techniques and methods [1]. In combination with the CAD/CAM technologies, the development of the Blade Adaptive Machining and Repairing System (BAMRS) has become a new trend for blade processing in the future [1, 2]. Figure 1 depicts the workflow of BAMRS consisting of two primary functions. The first function is the adaptive processing of blank blade to obtain high-accuracy parts and the second is the repairing of defective blades. The process aims at promoting cyclic utilization and green manufacturing.

The BAMRS is an effective tool to reduce the manufacturing cost in the blade repairing process. The basic steps of BAMRS are as follows: (1) measure the defective blade by measuring module of BAMRS to obtain the contour measured points, (2) reconstruct the defective blade model by using the measured points, (3) repair the defective region to obtain a repaired model, and (4) subsequent machining operations involving additive manufacturing, tool path planning, generating NC code, machining simulation, and actual machining. In the above steps, the defective blade repair using measured points and the reconstruction model are the most significant steps to realize the repairing function in the BAMRS.

In the blade working process, the different types of blade defects usually include fracture, surface damage, erosion, and cracks [3], thereby causing the blade surface to be incomplete. Moreover, the blade deforms completely under the impact of an airflow shock, making the nominal model inapplicable for repairing [4]. Therefore, the blade repairing based on measured points becomes a significant issue.

Blades, especially aero-engine blades, are high-precision parts. The profile accuracy of a blade surface plays a decisive

✉ Hongying Yu
mcadyhy@hit.edu.cn

✉ Xuegeng Lyu
xuegeng12@hit.edu.cn

[1] School of Mechatronic Engineering, Harbin Institute of Technology, Harbin, People's Republic of China

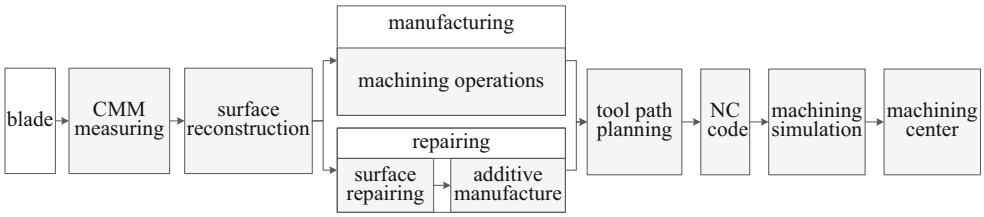

Fig. 1 Workflow of blade adaptive machining and repairing system

role in its performance, and slight changes in the blade profile may lead to significant changes in the aerodynamic performance. Therefore, a high-precision blade repairing model is necessary. There are two ways to achieve an increased repairing accuracy, and they are as follows: (1) improve the accuracy of measured points and (2) propose new repairing methods. In the method of acquiring points, the contact measurement method can achieve a high accuracy of 0.001 mm, while the non-contact method can only achieve 0.05 mm [5]. Therefore, the aforementioned points in relation with the contact method should be considered to obtain high-precision measured points; furthermore, increased efforts should be focused on proposing new repairing algorithms or methods to restore the original shape of the defective blade with the highest accuracy possible to ensure good aerodynamic performance.

Currently, scholars have accomplished some success in the blade surface repairing techniques. Section 2 discussed the literature available related to this research.

2 Related work

In order to repair a straight defective blade, the blade surface can be reconstructed by sweeping the same cross-sectional curve along a spatial direction. However, for a curved blade and a twisted blade, the repairing process is more complex. At present, most researches are aimed at curved or twisted blades; these methods can be classified into three categories.

The first method of blade repair is based on the reconstruction of the cross-sectional curves. Mohaghegh et al. [6] reconstructed the blade airfoils based on the designer's intent and proposed the seven arc methods to define the turbine blade airfoil section. The method separates the curves of the suction side, pressure side, leading edge, and trailing edge into several arcs. The authors argued that the algorithm could keep the geometry of the airfoil and filter the waviness of the profile. In a subsequent research, Mohaghegh et al. [7] presented a combined reverse engineering process that acquires information from two different sources, i.e., measuring the part and reviewing the design aspects, to capture the designer's intent as an alternative to copying every detail of the part. Rong et al. [8] studied a surface reconstruction strategy based on the profile's template. The method repaired the defective blade by the deformation of the template curve, which avoided data preprocessing such as sorting and parameterizations, during the process of blade repair. Bagci [2] studied the recovery application of reverse engineering through three examples. The author's research successfully proved the method to recover the defective blade without a 3D model, thereby displaying possibilities of use and benefits from utilizing the reverse engineering methodologies and techniques in the production process. Ng et al. [9] introduced a robust profile reconstruction (RPR) algorithm, which is a combination of the reference template and the lower section of the blade, used to predict and reconstruct each sectional layer. Wang et al. [10] studied a method to obtain the cross-section plane to repair tip-defective blade; the method involved 3D non-contact digitization and deduction of the damaged cross-sectional curve through the undamaged part. However, the method was suitable to repair a small-scale defective area only.

The second method of blade repair is based on the reconstruction and adaptive repairing of the defective blade surface. On the basis of a 3D optoelectronic sensor system, simulation and cutting path planning system, and a multi-axis high-speed milling center, Brinksmeir et al. [11] built an advanced maintenance system for turbine blade repair that realized the blade-reshaping by an adaptive milling technique. The Brinksmeir et al. method of applying reverse engineering had a significant influence in the field of blade repairing. On the basis of reverse engineering, Bremer [12] and Dix [13] studied the adaptive repairing solutions to achieve accuracy and repeatability. The authors used digitizing measurement techniques to collect 3D points and build a database in repairing systems. The methods involved increased human interaction and longer processing time instead of the automated adaptive solutions. Under the influence of adaptive repairing, other scholars have made a few exceptional achievements. The achievements of Gao and Yilmaz et al. [1, 4, 14, 15] are particularly prominent. The authors introduced a polygonal modeling approach and proposed adaptive restoration of complex geometry parts. Moreover, the authors also proposed a defect-free model-based repair strategy to generate correct tool paths for generating machining processes that were adaptive to each worn component [14]. In addition, the authors also studied geometry reconstruction solutions [1, 4] to create a worn component geometry and an advanced methodology for the repairing of complex geometry. The approach involves the integration of 3D non-contact digitization, adaptive free-form surface reconstruction, and multi-axis milling operation. Furthermore,

based on the available geometry of defective blade, Gao et al. [15] also presented a surface extension algorithm to calculate the unknown control points of the surface with the purpose of regenerating the geometry of the defective blade. Since numerous kinds of control points can be chosen in the process of surface extension, a possibility of a high level of uncertainty in the process of repairing the worn blade with a large-scale damaged area may exist.

In addition to the above two repairing categories, a few additional new algorithms have also been used for repairing the blade surface. Wang et al. [16] reconstructed the blade surface by point-cloud and envelope curves that were plotted from the approximate boundary points. These boundary points were obtained by the method of varied step lengths with respect to the curvature. In a subsequent research, a multi-scale genetic algorithm was used for fitting the edge of a turbine blade resulting in a 3D digital model reconstruction on its basis [17]. Piya et al. [18] considered a semi-automated geometric algorithm for virtually repairing defective blades. The algorithm was constructed by using the sectional gauss map to generate a series of prominent cross-sections along the longitudinal axis of the defective airfoil. The intrinsic geometry of the non-defective region is then extrapolated across the defective region to fill in the voids. Barbero [19] studied the issue through the recovery of the designer's intent instead of exploring the complex mathematical algorithm. The author took the recovery of a cam as an example to successfully demonstrate the research. However, the method based on designer's intent is more suitable for parts with a regular shape. Zheng et al. [20] studied the triangular patches growth method by point-cloud. However, the authors did not consider the topological continuity of a reconstruction model. In addition, Li et al. [21] studied the repairing issue by a 3D measuring method. The authors extracted the damaged region through a point-cloud by 4D Shepard surface based on the curvature estimation method. This research improved the efficiency of blade repair to an extent.

On reviewing the above researches, it can be observed that the recent repairing methods use point-cloud for repair, extracting reference points through the point-cloud, repairing cross-sectional curves, or directly repairing the blade surface through point-cloud. In fact, any blade repairing methods is a speculation in the absence of the theoretical CAD model and engineering documentation of the blade. The current repairing "guesswork" approaches seem to lack reasonableness. This lack of reasonableness will primarily lead to a great uncertainty on the repaired blade model; therefore, multiple blade models may be recovered through different methods and these blade models may differ on site. Moreover, the uncertainty of model repair cannot guarantee the accuracy of the repaired model. A few methods may have low repairing accuracy. In addition, the majority of the available literature only takes the fairing of the repaired blade surface as the final objective and the accuracy of the repaired model is not examined; therefore, the advantages and disadvantages of the algorithm or method cannot be measured.

In view of the above reasons, to improve the accuracy of repaired blade model as much as possible and to restore the original shape of the blade, increased attention should be paid to new algorithms and methods that aim at improving the rationale of the restoration process and reducing the occurrences of uncertain repaired results. Therefore, considering the unique characteristics of the blade, the present authors studied a high-precision and reasonable repairing method of the defective 3D blade model, in the absence of the theoretical CAD model and engineering documentation of the blade.

The blade is a special part of any machine, for example, steam turbine blade and aero-engine blade. The blade surface has distinctive features, and the overall blade surface is formed by blending different cross-sectional curves at different heights. These cross-sectional curves show the following two characteristics: (1) The cross-sectional curves are similar in outline. (2) Along the longitudinal direction of the blade, if the two cross-sectional curves are close, then the similarity is higher. The typical characteristics of blades, for example, a non-defective region or the repair of the defective area, would be useful for the improvement of the accuracy of the reconstruction model and reasonable repair. Therefore, the present authors propose a new method of deforming the reference cross-sectional curve adjacent to defective cross-sectional curve recursively to repair the defective region. The method includes four steps. Since the blade surface is obtained by skinning the layered cross-sectional curves, the first step is to divide the defective region into several layers along the height of the blade. In the second step, the defective region is repaired by the non-defective region. Therefore, from the first step, a non-defective cross-sectional curve adjacent to the defective region should be considered as the reference curve that would be deformed to restore the defective cross-sectional curve. The defective cross-sectional curve should have a certain rotation angle in the direction of blade height, due to the reference curve; therefore, it is necessary to register the projected direction of the blade height. The registration is accomplished by listing the measured points of the defective curve and the reference curve. In the third step, the reference curve and measured points of the first defective cross-sectional curve are registered. Consequently, the first defective cross-sectional curve is repaired by the deformation of the reference curve. Subsequently, the former repaired defective cross-sectional curve is assumed as the reference curve and the next defective cross-sectional curve is repaired. The process is repeated until all the defective cross-sectional curves are completely repaired. In this method, the repair of the defective cross-sectional curves enables the inheriting of characteristics of the adjacent cross-sectional curves; this effectively avoids uncertainty in the process of repairing. Moreover, the accuracy

of the repaired surface is enhanced to a certain degree by adapting contact measured points. Figure 2 displays the overall flowchart of the proposed new method.

In previous studies, the surface reconstruction for a thin blade from disorganized contact measured points was achieved [5]. On the basis of the aforementioned, the repairing method of the defective blade was studied. This paper is organized as follows: Section 1 is the introduction of the main research content. Section 2 is the related work conducted in at an early stage. Section 3 discusses the interpolation algorithm of the non-defective cross-sectional curves based on the contact measured points, and the determination criterion of the measured point density is presented in Section 4. Section 5 studies the registration of the reference curve and the measured points of the defective cross-sectional curve. Section 6 proposes reference curve deformation algorithm by an iterative distribution of the control points. Examples are studied in Section 7. And Section 8 presents the conclusion of the research work.

3 Interpolation algorithms of non-defective cross-sectional curve

The contact measured points can be obtained by CMM, and a reference curve can be interpolated by the non-defective cross-sectional curve points. B-spline and NURBS are the most popular choices for interpolation calculation. Since the subsequent repairing process performs the deformation operation on reference curve, it is necessary to investigate the deformation characteristics of B-spline and NURBS curve. The deformation of the B-spline curve is conducted by moving the control points, while the deformation in NURBS curve is done by modifying the control points and their weights. In order to obtain the same amount of curve deformation, the method of changing weights results in larger changes in weights compared to moving the control points. However, a significant change in the weight can lead to bad parametrization, which will lead to unexpected issues in the subsequent deformation process [22]. When the deformation is changed by modifying the control points, only the optimal control points are chosen to move, which are relatively stable. Therefore, the B-spline curve is used to interpolate the reference curve.

In the B-spline curve method, first, the relation between the number of measured points and the number of control points is determined. In a B-spline curve, the control points $\mathbf{d}_i (i = 0, \cdots, n)$, a total of $(n + 1)$ points, are set, and the knot vector is set as $\mathbf{U} = [u_0, u_1, \cdots, u_{n+k+1}]$, where k is the degree. In order to make the two ends of the curve coincide with the first and last control points, $u_0 = \cdots = u_k = 0$, $u_{n+1} = \cdots = u_{n+k+1} = 1$ is set. Further, set $\mathbf{q}_i (i = 1, \cdots, m)$, with m curve points. In the process of interpolation, $\mathbf{q}_i (i = 1, \cdots, m)$ corresponds to $u_k, u_{k+1}, \cdots, u_{n+1}$ respectively. Therefore, the following relationship exists between m and n:

$$n = m + k - 2$$

Given m curve points, it is necessary to determine from 0 to n ($=m + k - 2$, a total of $m + k - 1$) control points.

The expression of the B-spline curve is as follows:

$$\mathbf{p}(u) = \sum_{i=0}^{n} \mathbf{d}_i N_{i,k}(u)$$

where $N_{i,k}(u)$ are the B-spline basis function. In the case when the curve defined in $u \in [u_i, u_{i+1}]$, omitting the item whose basis function is 0, the B-spline curve can be expressed as follows:

$$\mathbf{p}(u) = \sum_{j=i-k}^{i} \mathbf{d}_j N_{j,k}(u)$$

Therefore, for m interpolation nodes, the expression is as follows:

$$\begin{cases} \mathbf{p}(u_i) = \sum_{j=i-k}^{i} \mathbf{d}_j N_{j,k}(u_i) = \mathbf{q}_{i-k+1} & (i = k, \cdots, n+1) \\ \mathbf{p}(u_{n+1}) = \sum_{j=n-k+1}^{n} \mathbf{d}_j N_{j,k}(u_i) = \mathbf{q}_m \end{cases} \tag{1}$$

including m equations and $(n + 1)$ variables.

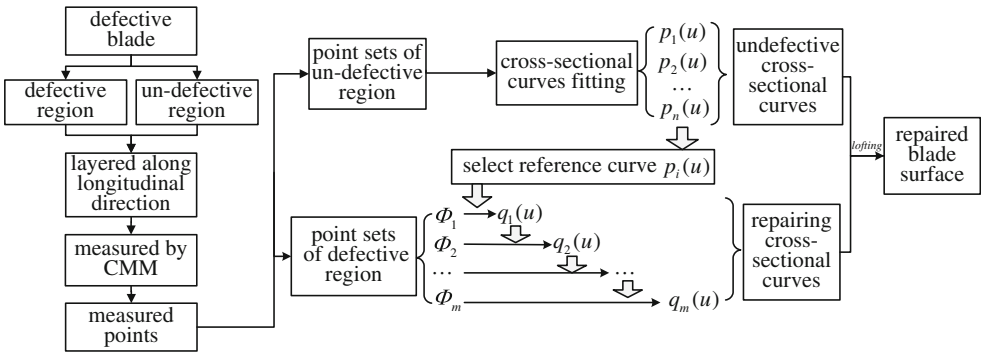

Fig. 2 Overall flowchart of blade surface repairing

The common interpolation uses $k = 3$. However, in the subsequent curve deformation operation, the influence interval of each control point is relatively small. The move of a single control point results in deformation of a small range of the curve. Therefore, a quintic B-spline curve($k = 5$) is used for interpolation. Equation 1 includes m equations and $m + 4$ variables; set $\mathbf{d}_0 = \mathbf{q}_1$, $\mathbf{d}_n = \mathbf{q}_m$ to ensure that the two ends of curve coincide with the first and last control points. In view of this, Eq. 1 would reduce two equations and two variables, leaving $(m - 2)$ equations and $(m + 2)$ variables. In order to solve the equation for the remaining control points, first- and second-order vectors of the two ends of the curve are added as the four boundary conditions. In consideration of the first and second derivatives of B-spline, the four boundary conditions can be derived as in Eqs. 2, 3, 4, and 5.

$$\mathbf{d}_1 = \frac{u_{k+1} - u_1}{k}\dot{\mathbf{q}}_1 + \mathbf{q}_1 \tag{2}$$

$$\mathbf{d}_{n-1} = \mathbf{q}_m - \frac{u_{n+k} - u_n}{k}\dot{\mathbf{q}}_m \tag{3}$$

$$a\mathbf{d}_1 + b\mathbf{d}_2 = e\ddot{\mathbf{q}}_1 + f\mathbf{q}_1 \tag{4}$$

$$c\mathbf{d}_{n-2} + d\mathbf{d}_{n-1} = g\ddot{\mathbf{q}}_m + h\mathbf{q}_m \tag{5}$$

where $a = -\left(\frac{u_{k+1} - u_2}{u_{k+2} - u_2} + \frac{u_{(k+1)} - u_{(2)}}{u_{(k+1)} - u_{(1)}}\right)$, $b = \frac{u_{k+1} - u_2}{u_{k+2} - u_2}$, $c = \frac{u_{n+k-1} - u_n}{u_{n+k-1} - u_{n-1}}$, cont. $d = -\left(\frac{u_{n+k-1} - u_n}{u_{n+k} - u_n} + \frac{u_{(n+k-1)} - u_{(n)}}{u_{(n+k-1)} - u_{(n-1)}}\right)$, $e = g = \frac{1}{k(k-1)}$, $f = -\frac{u_{k+1} - u_2}{u_{k+1} - u_1}$, and $h = -\frac{u_{n+k-1} - u_n}{u_{n+k} - u_n}$.

On combining Eq. 1 and Eqs. 2, 3, 4, and 5, a matrix equation (Eq. 6) can be obtained. The control points of the interpolation curve can be obtained by solving Eq. 6.

$$[N_{ik}] \cdot \mathbf{D} = \mathbf{Q} \tag{6}$$

where $\mathbf{D} = [\mathbf{d}_1, \mathbf{d}_2, \cdots, \mathbf{d}_{n-1}]^{\mathrm{T}}$,

$$\mathbf{Q} = \left[\frac{u_{k+1} - u_1}{k}\dot{\mathbf{q}}_1 + \mathbf{q}_1, e\ddot{\mathbf{q}}_1 + f\mathbf{q}_1, \mathbf{q}_2, \cdots, \mathbf{q}_{m-1} - \mathbf{q}_m \cdot N^n_{n,k}, g\ddot{\mathbf{q}}_m + h\mathbf{q}_m, \mathbf{q}_m - \frac{u_{(n+k)} - u_{(n)}}{k}\dot{\mathbf{q}}_m\right]^{\mathrm{T}}, \text{ and}$$

$$[N_{ik}] = \begin{bmatrix} 1 & & & & & & \\ a & b & & & & & \\ N^{k+1}_{1,k} & N^{k+1}_{2,k} & N^{k+1}_{3,k} & N^{k+1}_{4,k} & N^{k+1}_{5,k} & N^{k+1}_{6,k} & \\ & \ddots & \ddots & \ddots & \ddots & \ddots & \\ & & N^n_{n-5,k} & N^n_{n-4,k} & N^n_{n-3,k} & N^n_{n-2,k} & N^n_{n-1,k} \\ & & & & & c & d \\ & & & & & & 1 \end{bmatrix} \left(N^j_{i,k} = N_{i,k}(u_j)\right).$$

It should be noted that the above interpolation algorithm is applicable only for an open curve. However, the non-defective cross-sectional curve is a closed curve due to high computational efficiency caused by the number of interpolation curve points (measured points) that exceed 50. In case the closed cross-sectional curve is interpolated through all the measured points at one time, the calculated matrix would be larger than 50. As a result, in the subsequent repairing processes, a large matrix would always be associated with the registration of the reference curve and the measured points of defective cross-sectional curve including the iterative deformation of the reference curve. The repeated computations using a large matrix lead to an increased computation time, thereby resulting in a time-consuming process. Therefore, while interpolating the reference curve, the whole cross-sectional curve is divided into four parts: pressure-side curve, suction-side curve, inlet-edge-arc curve, and outlet-edge-arc curve. To significantly reduce the computing time of the calculation process, only the corresponding curve is involved in the calculation and other curves are only moved.

4 Determination criterion of measured point density

In the repairing process, if the defective region is large and limited to the local support property of the B-spline curve, the modified reference curve may not cover the entire defective region due to an inappropriate density of the measured points. Consequently, the measured point density will affect the accuracy of blade repairing. Therefore, when the deformation of the curve occurs at the closest point to the defective region, the deformation of a cross-sectional curve should cover the largest defective region to prevent a significant curvature change. As shown in Fig. 3, $\mathbf{q}_i$ and $\mathbf{q}_{i+1}$ are the point constraints; $\mathbf{p}_i$ and $\mathbf{p}_{i+1}$ are the closest points of $\mathbf{q}_i$ and $\mathbf{q}_{i+1}$ on the reference curve. When the $\mathbf{q}_i$ constraints are executed, the change in

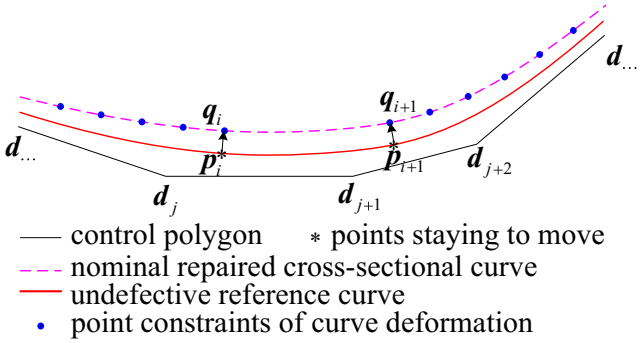

Fig. 3 Curve deformation constraints

the entire reference curve by the movement of $\mathbf{p}_i$ should include the part between $\mathbf{p}_i$ and $\mathbf{p}_{i+1}$, corresponding to the defective part $\mathbf{q}_i$~$\mathbf{q}_{i+1}$. Therefore, the present research studies the relationship between the density of measured points and the size of defective region. The determination criterion of the point density is depicted in Fig. 3.

The spline curve can be divided into several segments by its knot vector. The point $\mathbf{p}_i = \mathbf{p}(\tilde{u}) \in \mathbf{p}(u)$ $(\tilde{u} \in [u_t, u_{t+1}])$ is defined by the knot vector $U = [u_0, u_1, \cdots, u_{n+k+1}]$ and the control points $\mathbf{d}_i (i = 0, \cdots, n)$, and $\mathbf{p}_i$ is most associated with $k+1$ control points $(\mathbf{d}_{t-k}, \cdots, \mathbf{d}_t)$. Furthermore, for an arbitrary control point $\mathbf{d}_j (j = 0, \cdots, n)$, the movement of $\mathbf{d}_j$ will at most affect these curve segments defined on (u_j, u_{j+k+1}). Therefore, the movement of $\mathbf{p}_i$ on $\mathbf{p}(u)$ will change the curve shape on (u_{t-k}, u_{t+k+1}) (refer to Fig. 4), and a total number of $2k$ segment curves are affected.

Assume that the arc length of the corresponding reference curve period is l and the maximum width of defective region is l_0. Assume that m points will be taken on curve l at equal intervals. Therefore, $(m+k-1)$ control points will be obtained in accordance with Section 3. In the process of moving a single point $\mathbf{p}_i$ on $\mathbf{p}(u)$, which is closest to the defective region, the deformation of curve should cover the entire defective region. Thus, Eq. 7 should be satisfied.

$$2k\frac{l}{m-1} \geq l_0 \tag{7}$$

$$\boldsymbol{p}_i = \boldsymbol{p}\left(u\right)\left(u \in [u_t, u_{t+1}]\right) \Rightarrow \begin{cases} \boldsymbol{d}_{t-k} \begin{cases} u_{t-k} \\ \cdots \\ u_{t-k+k+1} \end{cases} \\ \cdots \{\cdots \\ \boldsymbol{d}_t \begin{cases} u_t \\ \cdots \\ u_{t+k+1} \end{cases} \end{cases}$$

Fig. 4 Influence range of executing a single point constraint

that is

$$m \leq \frac{2kl}{l_0} + 1 \tag{8}$$

Equation 8 gives the maximum value of the measurement point density. In Eq. 8, there is no requirement to determine the exact value of l and l_0; an approximately estimated value can be utilized. Moreover, the density of points can be increased appropriately in the larger curvature area of the blade surface.

It should be noted for the minimum value of m, a significantly lesser number of points will seriously affect the repairing accuracy. In general, m should be assumed to be at least half of the maximum points, that is $m \geq \frac{1}{2}\left(\frac{2kl}{l_0}, +, 1\right)$.

5 Registration of reference curve and measured points of defective cross-sectional curve

The repair of the defective cross-sectional curve is performed by the means of the deformation of the reference curve. However, in the direction of blade height, the projection of the defective cross-sectional curve and the reference curve show a certain rotation angle. When the reference curve is used for defective cross-section curve repair, registration between the reference curve and measured points of the defective cross-sectional curve is necessary. The repair of the defective curves based on registration not only inherits the characteristics of the adjacent reference curve but also limits the deformation of the reference curve to a small range, thereby avoiding unnecessary curvature mutation. In this study, the reference curve and measured points are registered through the features of the cross-sectional curves.

The aim of registration is to find the rotation matrix $\boldsymbol{R}$ and the translation matrix $\boldsymbol{T}$, to match the reference curve and defective curve under certain measured criterion. The registration is performed in two steps, the coarse registration and the precision registration. The following sub-sections detail the steps of finding the rotation matrix $\boldsymbol{R}$ and the translation matrix $\boldsymbol{T}$ by registration.

5.1 Coarse registration based on blade features

Coarse registration is implemented by the following steps.

Step 1: Preparation of cross-sectional curve. The interpolation algorithm of Section 3 enables the attainment of the reference curve (Γ) and defective cross-sectional curve (Γ') by utilizing the measured points of the non-defective and defective curves. A greater error may exist between Γ' and the desired repairing of the cross-sectional curve.

Since this step is a coarse registration, a high accuracy is not a requirement.

Step 2: Translation matrix $\mathbf{T}_{\mathbf{G}\to\mathbf{G}'}$. Discretize Γ and Γ' appropriately, and calculate their gravity center ($\mathbf{G}$, $\mathbf{G}'$) with respect to the discrete points. Establish the translation matrix $\mathbf{T}_{\mathbf{G}\to\mathbf{G}'}$ between $\mathbf{G}$ and $\mathbf{G}'$.

Step 3: Feature extraction. The following features were extracted from Γ and Γ': center point of the inner arc ($\mathbf{O}_1$, $\mathbf{O}_1'$), center point of the outlet arc ($\mathbf{O}_2$, $\mathbf{O}_2'$), chord length ($L\cdot\vec{e}_L, L'\cdot\vec{e}_{L'}$), and the maximum thickness of the blade ($\delta\cdot\vec{e}_\delta, \delta'\cdot\vec{e}_{\delta'}$). In accordance with the above characteristics, the following three groups of directions can be obtained: $\overrightarrow{\mathbf{O}_1\mathbf{O}_2}$ and $\overrightarrow{\mathbf{O}_1'\mathbf{O}_2'}$, $\vec{e}_L$ and $\vec{e}_{L'}$, and $\vec{e}_\delta$ and $\vec{e}_{\delta'}$. The defect of the blade may result in an inability to ascertain all the abovementioned three groups of directions; however, at least one group should be obtained. In case the above three groups of directions cannot be acquired, the blade is not expected to be repaired.

Step 4: Rotation matrix $\mathbf{R}_{\Gamma\to\Gamma'}$. The direction group is extracted in Step 3, and the gravity center obtained in Step 2 are considered as the original point to establish the rotation matrix $\mathbf{R}_{\Gamma\to\Gamma'}$ between Γ and Γ'.

Therefore, $\mathbf{T}_{\mathbf{G}\to\mathbf{G}'}$ and $\mathbf{R}_{\Gamma\to\Gamma'}$ are implemented on the measured points of the reference curve Γ in order to accomplish coarse registration.

5.2 Precise registration

On the basis of the coarse registration, the precision registration is implemented by the following steps.

Step 1: The measured point set of defective cross-sectional curve is assumed as $\mathbf{P}_1 = \{p_{1i}\}\ (i = 1, \cdots, N)$. The reference curve is assumed as Γ, and the control point set of Γ is assumed to be $\mathbf{Q} = \{q_i\}(i = 1, \cdots, N)$. Subsequently, solve the point set $\mathbf{P}_2=\{p_{2i}\}(i = 1, \cdots, N)$ that satisfies the condition $d(p_{2i}, \Gamma)=\min\limits_{p_{2i}\in\Gamma}\|p_{1i}-p_{2i}\|$.

Step 2: Set the mean distance function ε between $\mathbf{P}_1$ and $\mathbf{P}_2$: $\varepsilon = \frac{1}{N}\sum\limits_{i=1}^{N}\|p_{1i}-p_{2i}\|^2$. Thereafter, set the threshold value of ε: $[\varepsilon]$. The calculations should be stopped if $\varepsilon \le [\varepsilon]$, else the calculations should be continued by performing Step 3.

Step 3: The transformation matrix, including translation matrix $\boldsymbol{T}$ and rotation matrix $\boldsymbol{R}$, should "seek" to minimize ε between $\mathbf{P}_1$ and $\mathbf{P}_2$. The algorithm of "seeking" $\boldsymbol{T}$ and $\boldsymbol{R}$ used in this paper is the same algorithm that was used in [23].

Step 4: Set $\mathbf{Q}' = \mathbf{RQ} + \mathbf{T}$ and regenerate Γ. Thereafter, set $\mathbf{Q} = \mathbf{Q}'$ and return to Step 1.

Figure 5 illustrates the coarse and precise registration results of a reference curve and a defective cross-sectional curve. Figure 5a displays the original curves of reference and defective cross-sectional curves, the gravity centers of which are denoted by the red and blue points respectively. The coarse registration result is shown in Fig. 5b. A comparison of Fig. 5b with Fig. 5a shows that the overlapping of the reference curve and defective cross-sectional curve is increased. The precise registration result is shown in Fig. 5c. It is evident from the result that the two curves are almost coincident. However, when the part in the black rectangle is enlarged, a difference can be observed between the two curves (see Fig. 5d).

6 Iterative distribution algorithm of reference curve deformation

The registration lays a suitable foundation for the deformation reference curve. The deformation reference curve is required to pass through each measured point of the defective curve by moving its control points. This paper proposes an iterative distribution algorithm for the reference curve deformation to ensure a smooth deformation.

Firstly, the affine transformation of a point is introduced. Set $\mathbf{r} \in \varepsilon^3$ and define affine transformation $\Phi : \varepsilon^3 \to \varepsilon^3$, $\Phi(\mathbf{r}) = \mathbf{Ar} + \mathbf{V}$.

For a point ($u = \overline{u}$) on B-spline curve, set $\mathbf{r} = \mathbf{p}(\overline{u}) = \sum\limits_{i=0}^{n} N_{i,k}(\overline{u})\mathbf{d}_i = \sum\limits_{i=0}^{n}\alpha_i\mathbf{d}_i$ and $\sum\limits_{i=0}^{n}\alpha_i = 1$, where $\mathbf{d}_i$ ($\mathbf{d}_i \in \varepsilon^3$) are the control points. Then,

$$\begin{aligned}\Phi(\mathbf{r}) = \mathbf{Ar} + \mathbf{V} &= \mathbf{A}\left(\sum_{i=0}^{n} N_{i,k}\left(\overline{u}\right)\mathbf{d}_i\right) + \sum_{i=0}^{n} N_{i,k}\left(\overline{u}\right)\mathbf{V} \\ &= \sum_{i=0}^{n}\alpha_i(\mathbf{Ad}_i + \mathbf{V}) = \sum_{i=0}^{n}\alpha_i\Phi(\mathbf{d}_i)\end{aligned} \tag{9}$$

Equation 9 shows that the affine transformation of the B-spline curve can be changed by the position change of the control points. In the event that curve deformation occurs only under a point constraint, in Eq. 9, $\mathbf{A} = \mathbf{E}$ and $\overline{u} \in [u_t, u_{t+1})$; the control points, which affect the shape of curve at $\overline{u}$, are $\mathbf{d}_j (j = t-k, \cdots, t)$. Under the constraint $\mathbf{V}$, set the deformation curve of $\tilde{\mathbf{p}}(u)$ as $\tilde{\mathbf{p}}(u)$, then

$$\left|\tilde{\mathbf{p}}\left(\overline{u}\right)-\mathbf{p}\left(\overline{u}\right)\right| = |\mathbf{V}| = \left|\sum_{j=t-k}^{t}\alpha_j\mathbf{V}_e\right|\left|\mathbf{d}_j'-\mathbf{d}_j\right| = \left|\sum_{j=t-k}^{t}\alpha_j\mathbf{V}_e\right|\Delta d_j \tag{10}$$

$\mathbf{V}_e$ is the unit vector of $\mathbf{V}$.

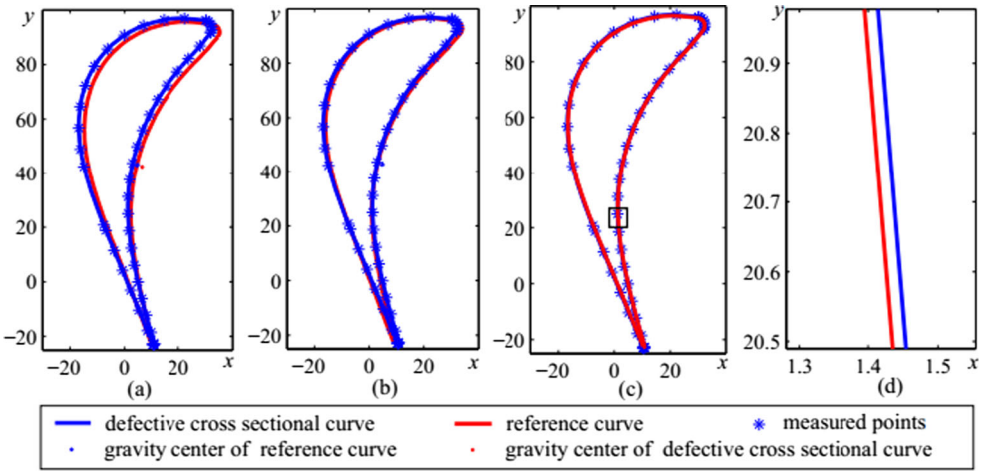

(a) Original curves; (b) Coarse registration result; (c) Precise registration result;

Fig. 5 Coarse and precise registration results of a reference curve and a defective cross-sectional curve. **a** Original curves. **b** Coarse registration result. **c** Precise registration result. **d** Enlarged figure of black rectangle in (c)

Eq. 10 denotes that if a curve is deformed by moving only one control point, then the moving distance $\Delta d_j = \frac{|\mathbf{V}|}{\alpha_j}$ $(j = t{-}k, \cdots, t)$ will be large. Therefore, the overall objectivity of the repaired curve will be defeated. Therefore, the deformation can only be implemented by moving all the control points associated with $\overline{u}$. Assigning the movement of a control point to all $\mathbf{d}_j (j = t-p, \cdots, t)$ could ensure the smoothness of the deformation curve.

After $\mathbf{d}_j (j = t-p, \cdots, t)$ are moved, the new control points are set to be $\tilde{\mathbf{d}}_j = \mathbf{d}_j + \gamma_j \alpha \mathbf{V}_e (j = t{-}k, \cdots, t$ and $\alpha = \frac{|\mathbf{V}|}{\sum_{j=t-p}^{t} \gamma_j N_{j,k}(\overline{u})})$. Subsequently, γ_j of $\tilde{\mathbf{d}}_j$ is determined.

In general, among all the control points set to move, $\mathbf{d}_p$, whose basis function is closest to $\overline{u}$, should have a larger moving distance, while other control points should assist $\mathbf{d}_p$ to move to ensure the entire curve is as smooth as possible without sudden bending. The parameter closest to the maximum of $N_{j,\ k}(u)$ for any basis function is as follows:

$$t_i = \frac{1}{k} \sum_{j=1}^{k} u_{i+j}, i = 0, 1, \cdots, n$$

t_i is denoted as a "node," which differs from "knot." Therefore, for the movement of $\overline{u}$ on curve$\mathbf{p}(u)$, the node vector $\mathbf{T} = [t_j]$ $(j = t-p, \cdots, t)$ and γ_j determination can be made with respect to the distance between $\overline{u}$ and t_j. The test verification shows that an improved default value of $\gamma_j$can be obtained as follows:

$$\gamma_j = \frac{\sum_{i=t-p}^{t} \frac{1}{|t_i - \overline{u}|}}{|t_j - \overline{u}|}$$

Therefore, $\tilde{\mathbf{d}}_j$ can be determined by $\mathbf{V}$, α, and γ_j. The defective cross-sectional curve can be repaired by the deformation of the reference curve using $\tilde{\mathbf{d}}_j$.

Figure 6 displays the repairing result of a defective cross-sectional curve. On enlarging the black rectangular part, the error between the nominal curve and the repaired curve can be observed. Figure 6a–c respectively represents the iteration times 1, 2, and 3. A comparison of the different iteration times is listed in Table 1. Table 1 shows that the error in the second iteration is much smaller than that in the first iteration, while the error in the third iteration is approximately equal to that in the second iteration.

After repairing a defective cross-sectional curve, the subsequent defective cross-sectional curve can be repaired by deforming the previously repaired cross-sectional curve. The above process is repeated until all the cross-sectional curves have been successfully repaired.

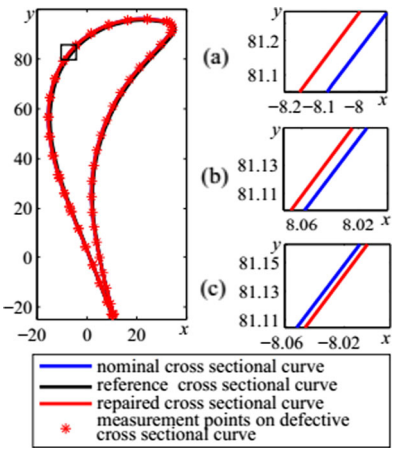

a) Iteration time=1; b) Iteration time=2; c) Iteration time=3;

Fig. 6 Repairing results of a cross-sectional curve after different iteration time. **a** Iteration time = 1. **b** Iteration time = 2. **c** Iteration time = 3

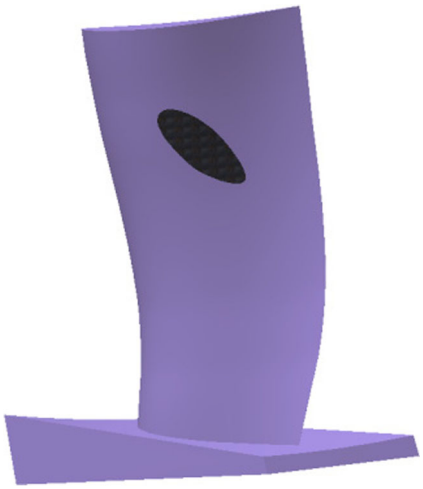

Fig. 7 Blade surface defective model

7 Repairing example of defective blade model

In order to prove the validity and innovation of the proposed method and to provide an effective blade surface repairing error map, a defectively designed blade CAD model was utilized as the repairing object. The repairing accuracy can be illustrated by an error map compared with the designed CAD model and the repaired model. The verification process is performed using the in Autodesk Inventor software. The secondary development functions of the Inventor are utilized to obtain the algorithm proposed in this paper by VB.net programming. Consider the following example.

Figure 7 shows the defective blade model. The measured points of the defective blade model have been obtained. In this example, the ratio l/l_0 (l_0 the width of the defective region; l the length of the suction side curve) is approximately 3.5. In accordance with Section 4, the measured point number is $m \in [18, 36]$. Assuming the value of m to be 21, the measured points of the defective region are shown in Fig. 8. Interpolate the first layer measured points to obtain the reference cross-sectional curve; thereafter, register the reference curve and the measured points of the second layer. Subsequently, the second defective cross-sectional curve is repaired by the deformation

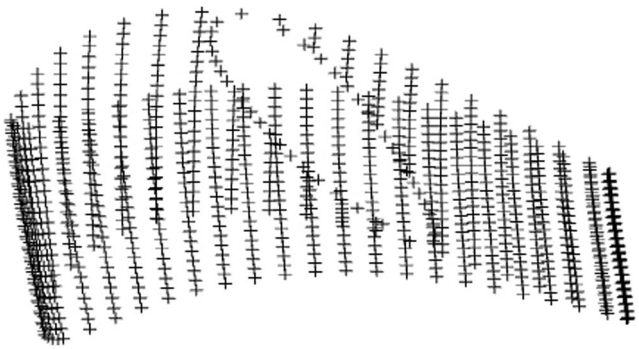

Fig. 8 Measured points of defective region

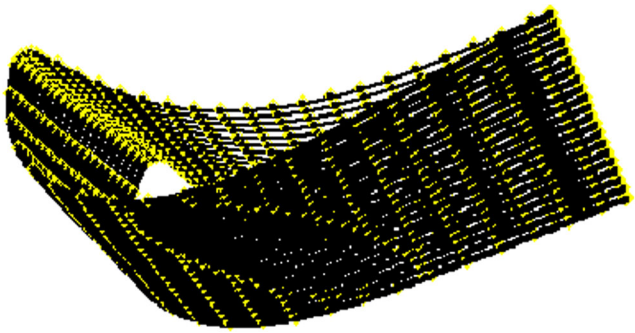

Fig. 9 Repaired cross-sectional curves

of the registration result. Thereafter, the second repaired cross-sectional curve is assumed as the reference curve for the next defective cross-sectional curve repairing process. The process of repair continues in this manner until the entire defective region has been repaired. Figure 9 displays the repair result of all defective cross-sectional curves. Subsequently, construct the repaired blade model by lofting these repaired cross-sectional curves and non-defective cross-sectional curves. Figure 10 presents the repaired blade model and an enlargement of the repaired cross-sectional curves.

In order to investigate the repairing effect, a comparison of the repaired surface and the designed surface of the blade is studied. As Fig. 11 shows, the normal error δ was selected as the error of point Q on repaired surface corresponding to point P on the designed surface. Figure 12 describes the error map of the pressure side surface of the repaired and designed blade model.

It can be observed from the error map of Fig. 12 that the maximum repairing error of the defective region is less than 25×10^{-3} mm. Furthermore, the repaired surface is much more accurate than the non-contact measured point-cloud repaired surface. Moreover, the most prevalent error occurs in the center of the defective zone. In comparison with the aforementioned value, the error of the marginal zone is lesser than that of the middle zone. The repair process is clear, simple, and easy to operate; in addition, the repair accuracy is high. Therefore, the proposed method can be used in BAMRS.

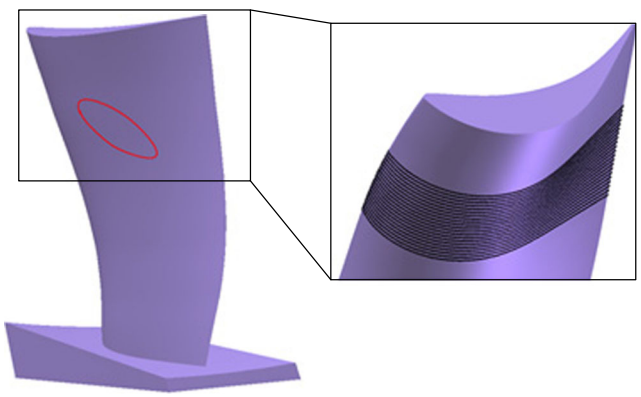

Fig. 10 Repaired blade model

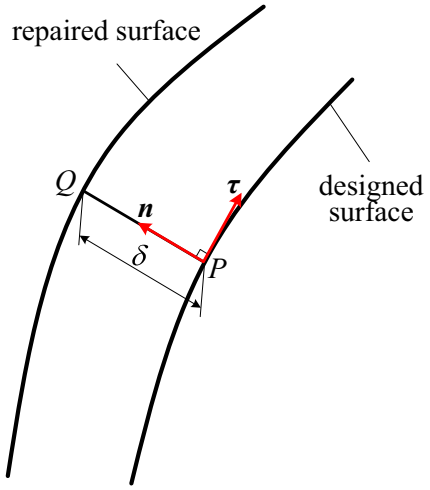

Fig. 11 Normal error

8 Conclusions and future works

In this paper, a high-accuracy repairing method for blade surface defect based on contact measured points was proposed. The conclusions that can be drawn are as follows:

1. Contrary to the previous method of blade repairing based on non-contact measuring point-cloud, the repairing was studied based on contact points. The advantages of blade typical characteristics were successfully utilized to propose a new method of deforming the reference cross-sectional curve adjacent to the defective cross-sectional curve recursively to repair the defective blade. The method of inheriting the characteristics of adjacent cross-sectional curves effectively reduces the uncertainty in the repair process.

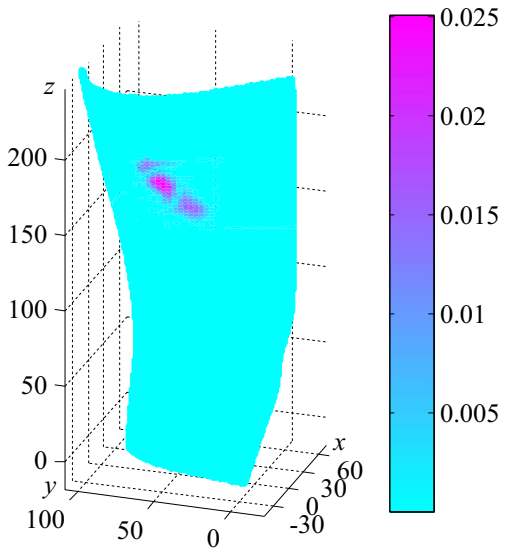

Fig. 12 Error map

Table 1 Comparison of different iteration times

Iteration time	1	2	3
Error (mm)	0.0643	0.0067	0.0057
Calculation time(s)	0.3780	0.7660	1.1430

2. A criterion for the determination of measured point density has been proposed in this paper based on the size relationship between the defective region and the entire cross-sectional curve. The appropriate contact point density ensures smoothness of the repaired blade surface.
3. A feature-based registration algorithm of reference curve and measured points of the defective cross-sectional curve has been presented to assist in defining the deformation reference curve. On the basis of registration, a method of iteratively moving the distribution algorithm of all the control points has been proposed to realize the repair of the defective blade.
4. The repairing example studied in this paper and the comparison between the repaired and designed models illustrate the validity and the degree of advancement of the proposed method. The method can successfully provide effective solutions for high-accuracy repairing of twisted blades. Additionally, the repairing method offers suitable conditions for CAD/CAM in several design and repairing cases.

This paper primarily studies a high-accuracy repairing method for a blade surface defect. However, the partial loss defect differs from surface defect. Moreover, the repairing of a twisted blade is further complicated. Therefore, our future research will focus on seeking a high-accuracy method of repairing partial loss defect twisted blade under limited measured points to perfect the defective blade repairing method.

Funding The author(s) disclosed the receipt of the following financial support for the research, authorship, and/or publication of this article: This research work was supported by a technology company of China Aerospace Corporation (Grant No. MH2016072).

Compliance with ethical standards

Conflict of interest The authors declare that they have no conflict of interest.

References

1. Yilmaz O, Gindy N, Gao J (2010) A repair and overhaul methodology for aeroengine components. Robot Comput Integr Manuf 26(2):190–201. https://doi.org/10.1016/j.rcim.2009.07.001
2. Bagci E (2009) Reverse engineering applications for recovery of broken or worn parts and re-manufacturing: three case studies. Adv Eng Softw 40(6):407–418. https://doi.org/10.1016/j.advengsoft.2008.07.003

3. Mazur Z, Garcia-Illescas R, Aguirre-Romano J, Perez-Rodriguez N (2008) Steam turbine blade failure analysis. Eng Fail Anal 15(1): 129–141. https://doi.org/10.1016/j.engfailanal.2006.11.018
4. Gao J, Chen X, Yilmaz O, Gindy N (2008) An integrated adaptive repair solution for complex aerospace components through geometry reconstruction. Int J Adv Manuf Technol 36(11–12):1170–1179. https://doi.org/10.1007/s00170-006-0923-6
5. Lyu X, Yu H, Wu J (2017) Surface reconstruction for thin aero engine blade from disorganized contact measured points. Proc Inst Mech Eng C J Mech Eng Sci:095440621769200. https://doi.org/10.1177/0954406217692007
6. Mohaghegh K, Sadeghi MH, Abdullah A (2007) Reverse engineering of turbine blades based on design intent. Int J Adv Manuf Technol 32(9):1009–1020. https://doi.org/10.1007/s00170-006-0406-9
7. Mohaghegh K, Sadeghi MH, Abdullah A, Boutorabi R (2010) Improvement of reverse-engineered turbine blades using construction geometry. Int J Adv Manuf Technol 49(5–8):675–687. https://doi.org/10.1007/s00170-009-2409-9
8. Rong Y, Xu J, Sun Y (2014) A surface reconstruction strategy based on deformable template for repairing damaged turbine blades. Proceed Inst Mech Eng, Part G: J Aerosp Eng 228(12):2358–2370. https://doi.org/10.1177/0954410013517091
9. Ng BT-J, Lin W-J, Chen X, Gong Z, Zhang J (2004) Intelligent system for turbine blade overhaul using robust profile reconstruction algorithm. Paper presented at the 8th International Conference on Control, Automation, Robotics and Vision, Kunming, China, Dec 6-9
10. Wang T, Ding H, Wang H, Tang J (2015) Virtual remanufacturing: cross-section curve reconstruction for repairing a tip-defective blade. Proc Inst Mech Eng C J Mech Eng Sci 229(17):3141–3152. https://doi.org/10.1177/0954406214567135
11. Brinksmeier E, Berger U, Janssen R (1998) Advanced mechatronic technology for turbine blades maintenance. Paper presented at the First IEE/IMechE International Conference on Power Station Maintenance—Profitability Through Reliability, Edinburgh, UK, march 30 -April 1
12. Bremer C (2000) Adaptive strategies for manufacturing and repair of blades and Blisks. Paper presented at the Manufacturing Materials and Metallurgy; Ceramics; Structures and Dynamics; Controls, Diagnostics and Instrumentation; Education, Munich, Germany, May 8–11
13. Dix B (2004) Aerofoil machining and polishing combined into a single automated process. Int J Aircr Eng Aerosp Technol 76 (5). https://doi.org/10.1108/aeat.2004.12776eab.005
14. Gao J, Chen X, Zheng D, Yilmaz O, Gindy N (2006) Adaptive restoration of complex geometry parts through reverse engineering application. Adv Eng Softw 37(9):592–600. https://doi.org/10.1016/j.advengsoft.2006.01.007
15. Gao J, Wen H, Wu H, Lin Z, Li S, Chen Y, He Y (2017) Geometric model reconstruction through a surface extension algorithm for remanufacturing of twist blade. Rapid Prototyp J 23(2):382–390. https://doi.org/10.1108/rpj-11-2015-0179
16. Wang T, Wang LW, Liu YL, Wang H, Tang J (2012) Digitally reverse modeling for the repair of blades in aero-engines. Appl Mech Mater 141:258–263. https://doi.org/10.4028/www.scientific.net/AMM.141.258
17. Wang LW, Wang H, Cai ZJ (2012) 3D model reconstruction of the broken aeroengine blade based on multi-scale genetic algorithm. Adv Mater Res 479-481:2250–2254. https://doi.org/10.4028/www.scientific.net/AMR.479-481.2250
18. Piya C, Wilson JM (2011) Virtual repair geometric reconstruction for remanufacturing gas turbine blades. Paper presented at the ASME 2011 International Design Engineering Technical Conferences and Computers and Information in Engineering Conference, Washington, DC, USA, August 28–31
19. Barbero BR (2009) The recovery of design intent in reverse engineering problems. Comput Ind Eng 56(4):1265–1275. https://doi.org/10.1016/j.cie.2008.07.023
20. Zheng J, Li Z, Chen X (2006) Worn area modeling for automating the repair of turbine blades. Int J Adv Manuf Technol 29(9–10): 1062–1067. https://doi.org/10.1007/s00170-003-1990-6
21. Li J, Yao F, Liu Y, Wu Y (2010) Reconstruction of broken blade geometry model based on reverse engineering. Paper presented at the The Third International Conference on Intelligent Networks and Intelligent Systems, Shenyang, China, Nov 1–3
22. Piegl L, Tiller W (1997) The NURBS book, 2nd edn. Springer, Berlin Heidelberg NewYork. https://doi.org/10.1007/978-3-642-59223-2
23. Besl PJ, McKay ND (1992) A method for registration of 3-D shapes. IEEE Trans Pattern Anal Mach Intell 14(2):239–256. https://doi.org/10.1109/34.121791